AFRL-RX-WP-TP-2010-4063

ELECTRONIC STRUCTURE METHODS BASED ON DENSITY FUNCTIONAL THEORY (PREPRINT)

Christopher F. Woodward

Metals Branch
Metals, Ceramics & NDE Division

JANUARY 2010

STINFO COPY

AIR FORCE RESEARCH LABORATORY
MATERIALS AND MANUFACTURING DIRECTORATE
WRIGHT-PATTERSON AIR FORCE BASE, OH 45433-7750
AIR FORCE MATERIEL COMMAND
UNITED STATES AIR FORCE

REPORT DOCUMENTATION PAGE

The public reporting burden for this collection of information is estimated to average 1 hour per response, including the time for reviewing instructions, searching existing data sources, gathering and maintaining the data needed, and completing and reviewing the collection of information. Send comments regarding this burden estimate or any other aspect of this collection of information, including suggestions for reducing this burden, to Department of Defense, Washington Headquarters Services, Directorate for Information Operations and Reports (0704-0188), 1215 Jefferson Davis Highway, Suite 1204, Arlington, VA 22202-4302. Respondents should be aware that notwithstanding any other provision of law, no person shall be subject to any penalty for failing to comply with a collection of information if it does not display a currently valid OMB control number. **PLEASE DO NOT RETURN YOUR FORM TO THE ABOVE ADDRESS**.

1. REPORT DATE *(DD-MM-YY)*	2. REPORT TYPE	3. DATES COVERED *(From - To)*
January 2010	Book Chapter Preprint	01 January 2010 – 01 January 2010

4. TITLE AND SUBTITLE	5a. CONTRACT NUMBER
ELECTRONIC STRUCTURE METHODS BASED ON DENSITY FUNCTIONAL THEORY (PREPRINT)	In-house
	5b. GRANT NUMBER
	5c. PROGRAM ELEMENT NUMBER 62102F

6. AUTHOR(S)	5d. PROJECT NUMBER
Christopher F. Woodward (AFRL/RXLMD)	4347
	5e. TASK NUMBER RG
	5f. WORK UNIT NUMBER M02R1000

7. PERFORMING ORGANIZATION NAME(S) AND ADDRESS(ES)	8. PERFORMING ORGANIZATION REPORT NUMBER
Metals Branch (AFRL/RXLM) Metals, Ceramics & NDE Division Materials and Manufacturing Directorate, WPAFB, OH 45433-7750 Air Force Materiel Command, United States Air Force	AFRL-RX-WP-TP-2010-4063

9. SPONSORING/MONITORING AGENCY NAME(S) AND ADDRESS(ES)	10. SPONSORING/MONITORING AGENCY ACRONYM(S)
Air Force Research Laboratory Materials and Manufacturing Directorate Wright-Patterson Air Force Base, OH 45433-7750 Air Force Materiel Command United States Air Force	AFRL/RXLMD
	11. SPONSORING/MONITORING AGENCY REPORT NUMBER(S) AFRL-RX-WP-TP-2010-4063

12. DISTRIBUTION/AVAILABILITY STATEMENT
Approved for public release; distribution unlimited.

13. SUPPLEMENTARY NOTES
Submitted for publication as a chapter in the ASM Handbook, Volume 22A: Fundamentals of Modeling for Metals Processing, 2010. PAO Case Number: 88ABW-2009-3258; Clearance Date: 16 Jul 2009. Paper contains color.

14. ABSTRACT
Over the last two decades electronic structure methods, based on Density Functional Theory, have emerged as a powerful tool for assessing the mechanical, thermodynamic and defect properties of metal alloys. These "First Principles" methods are very appealing because they are based on the culmination of our understanding of quantum mechanics and the electron-ion manybody problem. While the starting point for such calculations requires only the most a basic knowledge of chemistry, crystalline and defect structure the calculations can quickly become very computational challenging with increasing system size and complexity. Practical application of electronic structure methods invariably includes chemical, spatial or temporal approximations that can curtail a faithful representation of the actual materials problem.

15. SUBJECT TERMS
Density Functional Theory, quantum mechanics, spatial

16. SECURITY CLASSIFICATION OF:			17. LIMITATION OF ABSTRACT:	18. NUMBER OF PAGES	19a. NAME OF RESPONSIBLE PERSON (Monitor)
a. REPORT Unclassified	**b. ABSTRACT** Unclassified	**c. THIS PAGE** Unclassified	SAR	32	Christopher F. Woodward
					19b. TELEPHONE NUMBER *(Include Area Code)* N/A

Electronic Structure Methods based on Density Functional Theory
Christopher Woodward
Materials and Manufacturing Directorate
Air Force Research Laboratory

Introduction

Over the last two decades electronic structure methods, based on Density Functional Theory, have emerged as a powerful tool for assessing the mechanical, thermodynamic and defect properties of metal alloys. These "First Principles" methods are very appealing because they are based on the culmination of our understanding of quantum mechanics and the electron-ion many-body problem. While the starting point for such calculations requires only the most a basic knowledge of chemistry, crystalline and defect structure the calculations can quickly become very computational challenging with increasing system size and complexity. Practical application of electronic structure methods invariably includes chemical, spatial or temporal approximations that can curtail a faithful representation of the actual materials problem. However, over the last decade there have also been significant advances in methods for calculation free energies (entropy)[1], activated states (i.e. kinetics)[2], flexible boundary conditions[3], lattice dynamics[4], and reaction rate theory[5]. Taken with the rapid improvements in computer processor speeds and the maturation of "easy-to-use" DFT methods there has been an explosive growth in the use of DFT methods in materials science.

This Chapter is meant to be a guide to understanding the origins of these methods, their strengths and limitations and provide the basic procedures for calculating essential structural properties in metal alloys. Before delving into the details for DFT it is important to place the method in the context of the larger community of scientists interested in the nature of the electronic state in materials. Modern electronic structure emerged from method development in the Chemistry and the Physics communities and fall roughly into two groups: Hartree Fock and its extensions (HF+E) and Density Functional Theory. Historically, HF+E was been considered to be more precise, and has been preferred by Physical Chemists, because systematic improvements to the original approximation are well defined. For several reasons HF+E is not well suited for metallic systems, as will be discussed in detail in section N.1, and corrections to HF are extremely computationally intensive, scaling with the 4th to 6th power of the number of electrons. Density Functional Theory has been widely used in metallic systems since it's inception in 1962. With improvements in efficiency (speed) and refinements in the underlying approximations DFT is increasingly being used in Quantum Chemistry applications. Recently researchers have begun to blur the line between these two approaches by constructing novel potentials blending fundamental aspects of the two theories[6]. The resulting approximations show great promise for calculations over a broad range of problems ranging from atoms and molecules to chemically complex metal-oxide interfaces.

For scientists and engineers considering using electronic structure methods, navigating the sea of DFT acronyms can be challenging. In general the acronyms refer to the numerical scheme, or basis, used to represent the electrons. More recently, as methods have matured codes have been named after the groups that developed or support the method. All electronic structure methods must deal with the large changes in the electron distribution observed in atoms, molecules and

solids. Some of the electrons are strongly bound to the nuclear sites (core states) and are very similar to that found in isolated atoms. Others are more weakly bound (valence states) producing bonding, and are responsible for most of the electronic, optical, thermodynamic and chemical properties. Electronic structure methods deal with this disparity in a variety of ways, depending on what class of materials problem is under consideration. For example with isolated atoms and molecules it is natural to work in real space with methods based on a linear combination of atomic orbitals (LCAO), represented numerically or as a sum of analytic functions (e.g. gaussians). For crystalline systems it is more natural to use periodic boundary conditions and electrons are represented using a linear combination, or basis, of plane waves. Over time several methods were developed to avoid the large number of planewaves needed to represent the rapidly varying electron core densities. One approach, employed in augmented plane wave (APW) and muffin tin orbital (MTO) methods, is to use a set of local functions centered around each atom and to match that solution on a sphere to a plane wave basis everywhere else. Another technique, the pseudopotential method, maps the strongly bound electron states into a potential that is then used to calculate the valence electrons. These Pseudopotential Plane Wave (PPW) methods are relatively easy to use and the simplicity of the basis has allowed significant progress in computational efficiency (i.e. parallel processing) and analytic solutions for properties such as atomic forces and stress.

Historically mixed basis methods (APW, MTO) have been considered as the benchmark for accuracy in most applications. However, the mixed basis makes these methods more challenging to use and adds significant complications to deriving basic quantities such as atomic forces or stress. With advances in pseudopotential theory since the mid 1980's PPW methods routinely reproduce the results of mixed basis methods. Also, because of the added benefits of larger simulation sizes, automated atomic and cell optimization it can be argued PPW methods are producing more accurate results is wider range of applications.

Mixed basis methods are still the preferred technique for systems where the pseudopotential approximation breaks down. This happens when changes in valence electrons change the structure of the core electrons. For example in the actinides, where the f-electrons are coupled to the core states, APW and MTO methods are preferred[7]. Also, simulations of photo absorption and emission are probably best modeled using techniques where the core states are optimized along with the valence states. The quality and availability of pseudopotentials in some software packages can be quite limited. Researchers new to the field should carefully assess the available options before investing time or resources in any particular method.

One additional criterion to consider is the scale of the problem that needs to be solved. Inevitably this dictates the method and the required computational platform. Both LCAO and PW pseudopotential methods scale well on current parallel supercomputers and are typically applied to molecular and crystalline problems respectively.

DFT is being applied throughout the scientific community to a staggering range of problems. With current multi-processor supercomputers PPW methods can simulate system sizes up to approximately 1000 atoms[8]. This varies with the system symmetry and the choice of atomic species, with the transition metals being the most challenging. Researchers are also running ab-initio molecular dynamics simulations for cells ranging from 100-500 atoms for simulation times

up to tens of pico-seconds. The future of DFT will be driven by improvements to the underlying approximations, the introduction of new hybrid potentials, and advances in supplementary methods the use employ DFT results. Research into new novel basis functions (e.g. wavelets), or the introduction of new computer hardware (e.g. Field Programmable Gate Arrays) could revolutionize the field. Finally, while still in it's infancy there is a significant effort underway to directly calculate the electronic state by Quantum Monte-Carlo methods, if properly coupled to next generation supercomputers this eventually could overtake all other developments[9].

The rest of this chapter is divided into three independent sections. The first reviews the general underlying theory of electronic structure methods and Density Functional Theory specifically and the taxonomy of DFT methods that have emerged over the last thirty years. The second section reviews the approximations and computational details of the most popular method used in metal systems, the pseudopotential plane wave methods. The last section reviews a subset of the applications of DFT methods have found in metals alloy systems. This includes calculations of a variety of structural, thermodynamic and defect properties with particular emphasis on structural metal alloys and their derivatives.

N.1 The Fundamentals of Density Functional Theory:

We would like to model a chunk of matter using only what we know about coulomb interactions between electrons and ions and the underlying principles of quantum mechanics. The approach taken over the last 50 years has been to systematically apply approximations making the many-body problem more manageable while retaining the essential physics. Part of this evolving approach is to reduce the systems of equations to that subset which captures the problem of interest. We are not interested in solving systems with Avogadro's number of particles; not only would solving such a problem be unfeasible, analyzing the results of such a calculation would be a herculean task. Therefore for practical reasons, both conceptual and computational, it is considered best practice to minimize the scale (spatial and temporal) of the electronic structure calculation. There are many good reviews Density Functional methods. For a general overview of the fundamentals see R. Martin's text, Electronic Structure, Basic Theory and Practical Methods[10]. Payne et al. review the general theory of Pseudopotential Plane Wave methods and many practical issues on applying these methods[11]. Many practical details of PPW and Augmented Planewave methods are reviewed in D. Singh's text Planewaves, Pseudopotentials and the Linearized Augmented Plane Wave Method[12].

Beginning from classical mechanics, the many body Hamiltonian of an ensemble of interacting atoms takes the form:

$$H_{Total} = \sum_{I}^{M} \frac{P_I^2}{2M_I}$$

$$+ \frac{1}{2}\sum_{I}^{M}\sum_{I \neq J}^{M} \frac{Z_I Z_J e^2}{|\boldsymbol{R}_I - \boldsymbol{R}_J|} + \sum_{i}^{m} \frac{p_j^2}{2m_e}$$

$$+ \frac{1}{2}\sum_{i}^{m}\sum_{j \neq i}^{m} \frac{e^2}{|\boldsymbol{r}_i - \boldsymbol{r}_j|} - \sum_{I}^{M}\sum_{i}^{m} \frac{Z_I e^2}{|\boldsymbol{r}_i - \boldsymbol{R}_I|} \qquad (1)$$

Where M_I, $\boldsymbol{P}_I$, Z_I and $\boldsymbol{R}_I$ are the mass, momentum, charge and position of the M possible ions and m_e, $\boldsymbol{p}_e$ and $\boldsymbol{r}_i$ are the mass, momentum and position of the m possible electrons. The Hamiltonian is then separated into two parts, a purely ionic part (the first two terms in equation 1) and an ion-electron part:

$$H_{Total} = H_{Ion}(\boldsymbol{R}_I) + H_{e-Ion}(\boldsymbol{R}_I, \boldsymbol{r}_i) \qquad (2)$$

From this point Materials Scientist can choose to represent $H_{e\text{-}Ion}$ by an effective potential which leads to the field of atomistic modeling, or to invoke Quantum Mechanics and solve the many body Schrödinger equation which leads to the field of electronic structure methods. The later are generally considered a more faithful representation of the many body problem, as the electrons are treated explicitly. Standard practice is to now apply the Born-Oppenheimer approximation. Given that the electron cloud responds much faster to an applied field than the ions ($m_e/M_I \ll 1$), we can decouple the nuclear and electronic motion and solve for the electron degrees of freedom with the ionic positions held fixed. Using separation of variables the Schrödinger equation corresponding to equation 1 can be divided into two parts:

$$H\Psi(\{\boldsymbol{R}_I, \boldsymbol{r}_i\}) = (H_e + H_{Ion})\Psi(\{\boldsymbol{R}_I, \boldsymbol{r}_i\}) = E\ \Psi(\{\boldsymbol{R}_I, \boldsymbol{r}_i\}) \qquad (3)$$

using $\Psi(\{\boldsymbol{R}_I, \boldsymbol{r}_i\}) = \Psi_e(\{\boldsymbol{R}_I, \boldsymbol{r}_i\})\Psi_{Ion}(\{\boldsymbol{R}_I\})$ produces two equations:

$(T_e + V_{e-e} + V_{e-I})\Psi_e(\{\boldsymbol{R}_I, \boldsymbol{r}_i\}) = E_e\Psi_e(\{\boldsymbol{R}_I, \boldsymbol{r}_i\})$ and $(T_I + V_{I-I} + E_e)\Psi_I(\{\boldsymbol{R}_I\}) = E_I\Psi_{Ion}(\{\boldsymbol{R}_I\})$ where T and V refer to the kinetic and coulomb potential terms for the electrons and ions and the eigenvalues (E_e coming from the separation of variables) incorporated as an effective potential for the ionic problem. The many body Schrödinger equation for the m electrons is:

$$H_e\Psi_e(\{\boldsymbol{R}_I, \boldsymbol{r}_i\}) = \sum_{i=1}^{m}\left(\frac{-\hbar^2}{2m}\nabla_i^2 - Ze^2 \sum_{I}^{M} \frac{1}{|\mathbf{r_i} - \mathbf{R_I}|_e} + \frac{1}{2}\sum_{i \neq j}^{m} \frac{e^2}{|\mathbf{r_i} - \mathbf{r_j}|}\right)\Psi_e(\{\boldsymbol{R}_I, \boldsymbol{r}_i\})$$

$$= E_e\Psi_e(\{\boldsymbol{R}_I, \boldsymbol{r}_i\})$$

Unfortunately this equation cannot be solved directly. Two approaches are taken to solve this system of equations the first, Hartree-Fock and it's extensions (HF+E), solves for the electron

wave-functions and the second, Density Functional Theory, solves for the charge density (Drs. W. Kohn and J.A. Pople split the Nobel Prize in Chemistry in 1998 for aspects of these contributions). The Hartree-Fock approach is attractive because the derivation allows for well-defined systematic (though costly) improvements to the initial approximation for the third term in equation (2) , these are sometimes called "post Hartree Fock methods". HF+E methods are used extensively in non-metallic systems, however they are poorly suited for metal systems for several reasons. First, significant corrections to the initial HF approximation are required to properly represent metal systems. Second, in free electron metals HF produces an intrinsic instability in the electron velocity (a logarithmic divergence in $d\varepsilon/d$k, where $\varepsilon(k)$ is the energy dependence of the electron as a function of wave vector k) at the Fermi surface[13].

Density Functional theory is based on two insights provided Hohenberg, Kohn and Sham in the early 1960's[14,15]. First, Hohenberg and Kohn proved that for the ground state of an interacting electron gas in an external potential the electron density, $\rho(r)$, can be treated as the total energy of a system of interacting electrons in an external potential (i.e. the coulomb potential produced by the atomic nuclei) and is given exactly as a functional of the ground state electronic density: $E = E(\rho)$. Here a functional is defined as a function of a function – in this case E is function of the electron density. While the *Hohenberg-Kohn theorem* shows that E(p) is a unique functional it does not provide a prescription on how to form the functional, so the usefulness of the theorem is dependent on finding sufficiently accurate approximations[14].

To this end Kohn and Sham suggested writing E as:

$$E[\rho] = T_s[\rho] + E_{ei}[\rho] + E_{II}[\rho] + E_H[\rho] + E_{xc}[\rho] \tag{4}$$

the functionals on the right representing the kinetic energy of a system of non-interacting electrons, the electron-ion interactions, the Hartree potential of electron-electron interactions, the ion-ion interactions and the exchange correlation functional respectively[15]. The functional are now integrals over space, i.e. the last two terms explicitly are:

$$E_H[\rho] = \frac{e^2}{2} \iint dr\, dr' \frac{\rho(r)\rho(r')}{|r-r'|} \tag{5}$$

$$E_{xc}[\rho] = \int dr\, \rho(r)\, \epsilon_{xc}(\rho(r)) \tag{6}$$

In the last term Kohn and Sham identified $\epsilon_{xc}(\rho(r))$ as the exchange and correlation energy/electron of a uniform electron gas of density ρ. This is the *local density approximation* (LDA) which assumes that given a sufficiently slowly varying density a function, ϵ_{xc}, can be defined which represents the effective potential of an electron surrounded by its own "mutual exclusion zone" consistent with the requirements of quantum mechanics.

Using the fact that the functional $E[\rho]$ is an energy minimum with respect to variations in ρ (the H-K theorem) they then derived single particle Schrodinger like equations that are sometimes referred to as the Kohn Sham equations:

$$\left\{ -\frac{\hbar^2}{2m}\nabla^2 - Ze^2 \sum_{I=1}^{N} \frac{1}{|r - R_I|} + e^2 \int \frac{\rho(r')}{|r - r'|} dr' + \mu_{xc}(\rho(r)) \right\} \phi_i(r) = \epsilon_i \phi_i(r) \qquad (7)$$

Where $\rho(r) = \sum_{i=1}^{m}|\phi_i(r)|^2$ with m equal to the number of occupied states (the number of electrons in the system) and $\mu_{xc}(\rho) = d(\rho\epsilon_{xc}(\rho))/d\rho$ which is identified as the exchange-correlation contribution to the chemical potential of a uniform gas of densityρ. The system of equations is solved self-consistently by assuming a $\rho(r)$ constructing the last two terms in the KS equations and then solving for $\rho(r)$ using $\phi_i(r)$. The total energy is given by:

$$E[\rho(r)] = \sum_{i=1}^{m} \epsilon_i - \frac{1}{2} \iint \frac{\rho(r)\rho(r')}{|r - r'|} dr dr' + \int \rho(r)\left[\epsilon_{xc}(\rho(r)) - \mu_{xc}(\rho(r))\right]dr \qquad (8)$$

The K-S equation maps the interacting many electron system to a set of non-interacting electrons moving in an effective potential of all the other electrons. The utility of the K-S equations rest in our ability to find reasonable approximations for the functional $E_{xc}[\rho]$. Fortunately this function has been studied in detail for the case of a uniform electron gas[16], and derived using Monte Carlo techniques[17] and parameterized for electronic structure calculations[18].

LDA has been surprisingly successful in predicting a variety of properties in metals. Lattice parameters are usually accurate to within ~1% and cohesive energies and elastic constants to within ~10%. The method is well suited for studying solids, perfect and defected crystals and is easily extended to include spin dependence, the Local Spin Density Approximation, which has been widely applied to ferromagnetic and anti-ferromagnetic systems[19]. LDA is also the starting point for a variety of improvements based on the local change in the electron density produced by the electron (the exchange-correlation hole). These Generalized Gradient Approximations have systematically improved the accuracy of DFT for problems in molecular systems and broadened the application base significantly (these are reviewed in the next section). However, currently the method is still not well suited for systems with large Van der Waals energies or systems sampling infinitesimally small electron densities such as a structures bounded by a vacuum.

Where DFT methods seem to diverge is in the spatial representation of the one-electron wave functions. The wide variety of methods reflects the fact that an accurate representation of the charge density has traditionally required specialized basis functions. The fundamental problem is that as the atomic number increases the additional atomic wave-functions are required, by the Pauli exclusion principle, to be orthogonal to existing lower lying wave-functions. To accomplish this, as the principle quantum number increases, the wave-functions take on a rapidly

varying radial form near the atomic center. Therefore, for a set of basis functions to accurately describe the electrons it must be able to both represent the rapidly varying function near atomic centers and the relatively smooth functional form outside that region.

Several strategies have been used to solve this problem. Techniques such as the Augmented Plane Wave, Muffin Tin Orbital and Korringa Kohn Rostoker methods use an efficient and compact basis to describe the wave-functions near the atomic centers[20,21,22]. An additional basis (typically plane-waves) is used to describe the wave-functions outside this region and various schemes are used to ensure a proper match of the wave-functions at the boundary between these two regions. These methods give a very accurate representation of the core region, while allowing some flexibility in the basis outside this region. Refinements to these techniques such as the Full potential Linearized Augmented Plane Wave (FLAPW) [23] and Full Potential Linearized Muffin Tin (FP-LMTO) [24] are currently considered to be the most accurate DFT methods, though the implementations are limited to relatively small cell sizes.

The seminal work on Orthogonal Plane-Wave methods led to the development of an alternative technique where the low lying (core) states are effectively removed from the calculation[25]. In this case an effective electron-ion potential, or pseudo-potential, is derived from an atomic electronic structure calculation. Pseudo-potentials incorporate the tightly bound wave-functions and ionic charge so that the potential produces the same electronic interactions as the original atomic calculation. In this way the core electrons, which do not normally influence materials properties, can be removed from the simulation. By construction the pseudo-potentials produce the same interaction with the valence electrons as the original all electron calculation (as measured through the electron scattering properties)[26]. Recent pseudo-potential schemes have relaxed this philosophy during the construction of the potential, only to re-impose the requirement when constructing the Kohn-Sham orbitals in the system of interest[27,28]. Pseudo-potentials also incorporate the effective potential produced by the Pauli exclusion principle such that the valence wave-functions are smooth functions in all space. Therefore it is natural to combine a plane-wave basis with the pseudo-potential representation in what we now call pseudo-potential plane-wave methods (PPW).

While the plane-wave basis is not as compact as that used in the LAPW methods, PPW methods have been easier to implement because of the simplicity of the plane-wave basis. It is relatively straightforward to calculate atomic forces (through the Hellmann-Feynman theorem), the stress tensor and phonon properties [29,30,31]. However, until the mid 1980's application of PPW methods were somewhat limited because of the size of the required plane-wave basis set. In 1985 Car and Parrinello showed how to simultaneously optimize both the electronic and ionic degrees of freedom by taking advantage of fast fourier transforms and the plane-wave basis[32]. Iterative diagonalization methods that have grown out of these insights have shown that by proper preconditioning of the Kohn-Sham wave-functions during the optimization procedure it is possible to directly minimize the Kohn-Sham energy functional[33]. This innovation stabilizes

the constrained optimization of Eq. 1 and has made it possible to run very large simulations relatively efficiently[11].

Figure 1. Schematic of the methods developed by the chemistry and physics communities to solve the materials many body problem. In general the DFT methods are the method of choice for calculations on metallic systems.
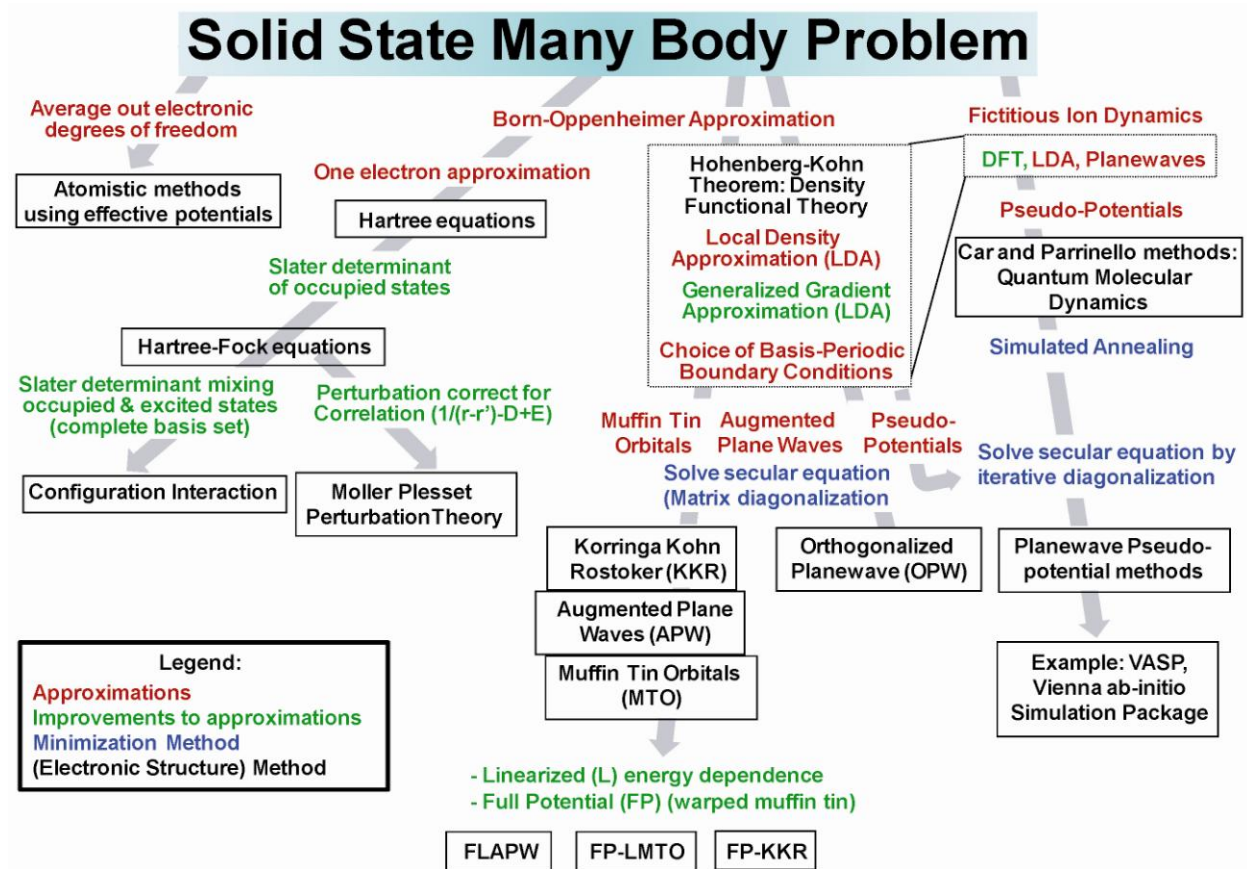
N.2 Pertinent Approximations and Computational Detail for Calculations in Metal Alloys:

In order to calculate the electronic structure of an alloy the researcher needs more than just an underlying theory and a working description (basis) of the electrons. First the methods need efficient and accurate techniques for integrating the quantities described in section 1 over the volumes (and k-space) of interest. Second, the approximations and basis need to be well matched to the problem of interest. Finally, explicit knowledge of the crystal structure, location and species of every atom on the simulation volume is required. Fortunately, for a most of the alloy of engineering interest this information is available in tabulations of the International Tables for Crystallography in the form of space groups, describing the symmetry of the lattice, and Wyckoff positions, describing the atomic sites (position and chemistry)[34].

Integration of cell quantities: One advantage to working on metallic systems is that the underlying crystalline structure is almost invariable periodic. This allows the researcher to employ simulation cells with periodic boundary conditions (supercells) to represent the material of interest. Periodic boundary conditions also make it possible to represent most all quantities of interest in terms of real and Fourier space (k-space) components. This is particularly useful when summing up terms numerically in the KS equations or equation (8) over the Brillouin zone.

The most straightforward way to integrate of quantities over the supercell is to divide the Brillouin zone using a tetrahedron grid of points (k-points). However, in the early 1970's numerical schemes were developed to predict the smallest set of k points, "special k-point", that would yield the most accurate cell integrations [35,36]. In most modern application codes the selection of k-points is sufficiently automated that the investigator needs to only input the required density of such points. However, one characteristic of a metal is that valence states, or bands, are partially occupied, and this can produce numerical instabilities. In order to avoid this and to improve the efficiency of the cell integration researchers introduced a numerical smearing of the highest lying bands, specifically those that are near the Fermi surface. The "broadening" methods fall into two classes, those employing ad-hoc functional forms such as Gaussians and finite temperature schemes based on the Fermi-Dirac or Gauss like functions that mimic thermal broadening [37,38]. Both methods are effective, and the latter technique has the advantage of an associated, if ad-hoc, temperature.

Computational time for metal simulations scales with the number of k-points, however as the simulation sizes get larger and reciprocal space get smaller the number of required k-points is reduced. For large simulations, say greater than 100 atoms, often only a single k-point is needed. Also, if only the gamma point (k = (0,0,0)) is required then calculations can gain another factor of 2 in efficiency, because of the symmetry imposed on the complex parts of the wavefunctions.

While there are rules of thumb for the use of special k-points and broadening methods, it pays to carefully test the convergence of such methods using, for example, the cell energy or other quantity of interest. In general the density of k-points should be approximately that of the size in dispersion in the bands near the Fermi surface[39].

Understanding and choosing a pseudopotential: Early in the development of electronic structure methods researchers realized that the electrons contained in full atomic shells (s, p and d) do not have a strong influence on chemical and mechanical properties. These effects are controlled mostly by the interaction of valence electrons, which have the largest principle quantum number, and thus the most rapidly varying radial function in the region around the atom nucleus. Pseudopotentials replace the core-valence electron interactions, the second term of equations (4) and (7), with an effective potential produces a realistic pseudo-valence wavefunction that has a smooth and slowly varying radial form. Typically pseudopotentials are derived from an atomic reference calculation and then used in crystalline or other environment, so transferability is a serious concern when developing such a scheme. Early local

pseudopotentials, and more recent implementations of the same, are severely limited and can only reliable be used in simple free electron metals where the core electrons have very weak interactions with the valence states[40.41].

Modern pseudopotential theory is based on a "norm-conservation" approach that enforces a strict criterion for mapping real to pseudo wavefunctions and includes non-local angular momentum (ℓ) dependent interactions that accurately model the valence-core electron interactions[26]. Transferability is maintained by imposing identical logarithmic derivatives, and thus scattering phase shifts, outside a certain (core) radius about each atomic site. More recent advances in pseudopotential theory such as Vanderbilt's ultrasoft pseudopotentials make use of additional functions about the atomic core, which allow for smoother pseudo wavefunctions and more efficient PPW calculations[27]. This and later refinements of pseudopotential theory parallel the original strategies used in Orthogonalized Plane Wave methods developed by Herring, Callaway and others from the mid 1900's[25]. The most recent advances in pseudopotential theory, the projector augmented wave (PAW) method[28], retains all the information of the core states and is thus analogous to the most accurate all electron methods (e.g. OPW, APW and MTO). Implementing the PAW methods in PPW codes required additional development and using the potentials incurs additional computational overhead.

Using modern numerical methods, current commercial PPW implementations of the PAW method are as efficient as the original Car and Parrinello methods and as accurate as many full potential methods. They have the added benefit of ease of calculation of atomic forces, stress tensor and convergence of basis. A wide variety of ultrasoft and PAW pseudopotentials are available in the user community as well as source code for developing such potentials. More importantly there are readily-available, well-documented suites of pseudopotentials that have been tested by a broad user base.

Exchange-Correlation Potentials, Local Density Approximation and the Generalized Gradient Approximation: Density Functional Theory is one of the most successful electronic structure methods precisely because of the simplicity of the underlying exchange-correlation functional. Practical application of the HK theorem through the KS equations requires a both an assessment of the exchange correlation functional and a numerically efficient scheme for interpolating the energy for a range of charge densities. Since the original formulation of the KS equations the nature of the exchange correlation potential has been studied in some detail. The Local Density Approximation is the foundation of all these approximations. Within the LDA only knowledge of the exchange correlation energy of the homogeneous electron gas is required. Thiis approximated as the sum of exchange and correlation potentials, the first given by a basic analytical form and the second calculated using Monte Carlo methods [17]. These data were then fit to functional forms to improve computational efficiency and parameterized for electronic structure calculations [18].

The Local Density Approximation has been found to be a surprisingly accurate in a wide variety of systems. The initial formulation was expected only to valid for volumes with slowly varying electron densities, a condition that is not well satisfied in many crystals. It is generally believed that the LDA approximation underestimates the exchange energy (by~10%) and overestimates the correlations energy (2%) and that these errors partially cancel each other out [42]. However, LDA is particularly unsatisfactory for low electron densities, such near a surface, and that has made the approximation problematic for calculations of atoms and molecules. Still, LDA produces reasonable accurate bond lengths and geometries for some molecules.

The efficacy of the KS equations and the need for highly accurate simulations has resulted in systemic improvements to the LDA. The most successful approaches, based on generalized gradient approximations (GGA), include information on the effects of inhomogeneities in the electron gas on the exchange correlation potential. The gradient corrections are constructed to satisfy intrinsic sum rules and are designed to maintain the accuracy of LDA while correcting the errors introduced by large gradients. Using FP-LMTO Ozolins and Korling calculated the changes in lattice constants and bulk modulus produced by using the GGA proposed by Perdew and Zhang (sometimes referred to as PW91)[43]. They found a systematic improvement in equilibrium volumes and bulk modulus for 3d, 4d, and 5d transition metals, with the mean error decreasing on average by 50% for both quantities across the series[44]. Other researchers also found that early GGA methods and PW91correctly produces the correct bcc ground state for crystalline Fe where the Local Spin Density Approximation erroneously predicts an fcc ground state [45.46].

Recently, other GGA methods are being validated that produce better energetics and better represent low density regions. Hybrid schemes based on a weighted mixing of HF exchange and DFT correlation have gained favor in the quantum chemistry community [47]. Also, another class of GGA functional has been self consistently matched to high and low electron densities, making it efficient and well suited for metallic systems with internal or external surfaces [48]

N.3 Practical Application of DFT in Metals and Alloys:

As illustrated in Figure N.2 DFT methods come in a variety of forms, they also vary widely in their level of maturity and efficacy. Until recently most of the mixed basis methods (FPLMTO and FLAPW) were closely held academic codes, now there are several freeware and commercial options (see Table 3). While highly accurate, these methods have a more complex set of adjustable basis parameters than PPW methods. There are a variety of PPW methods some available as freeware and some commercially, and some have well developed pseudopotential libraries. New users should verify a given code base has the necessary features for running their application before investing resources into a method. All of the methods shown in Table 3 should produce accurate results for the simple applications outlined in this section.

Table 3. Partial list of currently available DFT programs. Some are available for a license fee and others are available at no cost. Many of the methods have associated users groups and some have graphical user interfaces. Materials Science trade organizations are beginning to track the status of software (see for example: http://iweb.tms.org/forum) and may provide useful updates to this table.

Method	Acronym/Name	Fee	POC
PPW	ABINIT	No	http://www.abinit.org/, Prof. X. Gonze, Université catholique de Louvain, Physico-Chemistry and Physics of Materials, Louvain-la-Neuve, BELGIUM
	CASTEP	Yes	Accelrys, Inc., San Diego, CA 92121 http://accelrys.com/products/materials-studio
	Quantum Expresso: opEn Source Package for Research in Electronic Structure, Simulation, and Optimization	No	P. Giannozzi, Universit`a di Udine and Democritos National Simulation Center, Italy http://www.quantum-espresso.org
	VASP: Vienna Ab-initio Simulation Package	Yes	Prof. J. Hafner, Institute of Materialphysik Wien University Austria, http://cms.mpi.univie.ac.at/vasp/
LCAO	DMOL3	Yes	Accelrys, Inc, San Diego, CA 92121 http://accelrys.com/products/materials-studio
	SIESTA	Yes	Prof. J.A. Torres, Universidad Autonoma de Madrid, Spain http://www.icmab.es/siesta, http://www.nanotec.es/
FP-LMTO	LmtART	No	http://www.fkf.mpg.de/andersen/ S. Y. Savrasov, Phys. Rev. B 54, 16470 (1996).
	RSPt : Relativistic Spin Polarised (test)	No	http://www.rspt.net/index.php
FP-LAPW	WIEN2K	Yes	http://www.wien2k.at/index.html, Prof. Karlheinz Schwarz, Inst. f. Materials Chemistry, TU Vienna
	FLAIR		Prof. M. Wienert, Univ. Wisconsin Milwaukee, weinert@uwm.edu
	QMD-FLAPW	Yes	Prof. A.J. Freeman, Northwestern Univ. Quantum Materials Design, Inc., http://flapw.com/news.html

From crystal structure to input file, examples of VASP input files:

Setting up the simulation cell for electronic structure calculations requires: the lattice vectors, the atomic positions and the chemical species at each site. The input file required for the PPW method VASP will be used to illustrate this process [49,50]. Typically the researcher starts with a phase and then refers to tables and textbooks to find the required quantities. For example in Ni-

based superalloys Ni_3Al is an important precipitate that significantly strengthens the Ni matrix phase. Using the tabulated data on alloy phases in W.E. Pearson's Handbook of Lattice Spacings and Structures of Metals [51] the structure type is listed having a structure name (a representative material) $AuCu_3$, the Strukturbericht designation $L1_2$, a lattice parameter of 3.567 Angstrom, with a space group of $Pm3m$. The Pearson classification for $L1_2$, $AuCu_3$ is given as cP4 in the tables leading up to the Table of Classification of Structures of Metals and Alloys. A shortened version of the entry under cP4 is given in Table 4. After the first line describing the structure designations the atomic basis, the Wyckoff positions, are listed in terms of the atom type, the number of atoms at each symmetry distinct point and the internal coordinate. All the required information is now determined. The International Tables for X-Ray crystallography has more information for this cubic space group (number 221) and lists much more complicated crystal structures with this space group[34,52].

Table 4. Crystallographic information and atomic basis for $L1_2$, Ni_3Al.

Classification symbol	Structure name	Strukturbericht type	Space group
cP4	$AuCu_3$	$L1_2$	$Pm3m$
	Origin at center (m3m)		
	Equivalent positions:		
	Au: 1 a m3m 0,0,0		
	Cu: 3 c 4/mmm 0, ½,½; ½,0, ½; ½,½,0.		

The VASP the input file for the lattice vectors and atomic basis is called POSCAR and a screen shot of the POSCAR file for Ni_3Al is shown below. In POSCAR the title line is followed by the lattice constant from Pearson, the three lattice vectors for a cubic lattice in Cartesian coordinates. This is followed by the number of each chemical species, in this case 3 Ni atoms and one Al atom, and a keyword describing the format of the atomic basis. (Note that the order of the chemical species is important and must be consistent with the ordering of the pseudopotential input file.) The atomic basis can be entered in either Cartesian (Keyword: CARTESIAN) or in terms of the three lattice vectors (Keyword: DIRECT). For the "Direct" mode the atomic positions correspond to $\vec{R} = x_1\overrightarrow{a_1} + x_2\overrightarrow{a_2} + x_3\overrightarrow{a_3}$, where $\overrightarrow{a_i}$ are the lattice vectors scaled by the lattice parameter and x_i are the values entered into POSCAR. Input using the CARTESIAN keyword is scaled only by the lattice constant: $\vec{R} = x_1\hat{\imath} + x_2\hat{\jmath} + x_3\hat{k}$, where i, j, and k are unit vectors [100], [010], and [001] respectively.

Fig. 2. Screen shot of input file describing crystal system and atomic basis for γ'-Ni_3Al.

```
Example: Ni3Al           Title
3.57640                  lattice Constant (Ang.)
 1.00000  0.00000  0.00000  Lattice vector
 0.00000  1.00000  0.00000  Lattice vector
 0.00000  0.00000  1.00000  Lattice vector
3 1                      Number of each atomic species
Direct                   Format of the atomic positions
  0.000  0.500  0.500    Internal coordinates of atoms
  0.500  0.000  0.500
  0.500  0.500  0.000
  0.000  0.000  0.000
```

Another, more complex example of an atomic basis is the δ-MoNi phase, which is also important in the Ni-based superalloys. In Pearson this topologically closed packed phase is listed as orthorhombic with lattice constants: a=9.108, b=9.108, and c= 8.852 Ang., containing 56 atoms with the space group $P2_12_12_1$. Table 4 gives the representative atomic positions listed as 14 roman numbers with corresponding coordinates. The Wyckoff positions, listed in the International tables, for $P2_12_12_1$, are shown in Table 5. The atomic coordinates are generated by using the last column of Table 5 with each of the 14 atomic parameters producing the expected 56 atoms.

Table 4. Crystallographic information and atomic parameters for δ-MoNi [51].

Phase	System	Strukturbericht type	Space group					Est. % Mo[53]
δ-MoNi	Ortho-rhombic	-None-	$P2_12_12_1$	Atoms	Atomic parameters			
				IV	0.4519	0.1153	0.5322	0
				VI	0.4424	0.3662	0.5972	0
				VIII	0.3882	0.0523	0.2748	0
				IX	0.1337	0.0707	0.2157	0
				X	0.3768	0.4358	0.8567	0
				XII	0.0680	0.1442	0.9529	0
				I	0.1763	0.4832	0.6425	80
				XIII	0.0338	0.3398	0.1807	80
				II	0.2289	0.2865	0.4098	91
				V	0.2648	0.1993	0.7486	91
				XI	0.3136	0.2464	0.0740	58
				VII	0.0029	0.1969	0.6767	100
				XIV	0.1885	0.0157	0.4960	100
				III	0.1031	0.4192	0.9133	100

Note however the atomic species for each site is still unknown, going back to the original reference for this crystallographic assessment we can find the chemical assignments for most but not all the atomic sites[53]. At finite temperatures all alloys show deviations from perfect ordering, however the composition of the studied δ-MoNi phase was Mo49.2-Ni and X-Ray

14

analysis could not unambiguously determine the chemistry on at least one of the sites. The electronic structure calculations can proceed by assuming a Mo50-Ni composition and the chemistry at the sites designated by XI as being occupied by Ni atoms. This is however just one possibility, and in principle a free energy model would include sampling the formation energy of other atomic arrangements at this composition.

Table 5. Wyckoff Positions for Space group $P2_12_12_1$

Multiplicity	Wyckoff letter	Site Symmetry	Coordinates
4	a	1	$(x,y,z),(-x+\frac{1}{2},-y,z+\frac{1}{2}),(-x,y+\frac{1}{2},-z+\frac{1}{2}),(x+\frac{1}{2},-y+\frac{1}{2},-z)$

Using Tables 4 and 5 the initial cell was constructed as shown in the screen shot of the POSCAR file in Figure 3. The Figure also shows a screen shot of the final cell configuration. Using VASP the lattice vectors and atomic positions were optimized within a spin polarized (ferro-magnetic) ultrasoft pseudopotential approximation. Note the slight change in the length of the orthorhombic lattice vectors and the change in atomic positions. At the start of the calculation the pressure was ~ 16 kB and the largest force/atom was ~ 0.5 eV/Ang, after optimization the pressure was less than 0.5 kB and the atomic forces less than 2e-3 eV/Ang and the total energy change from the intial configuration was ~ 0.5 eV.

Figure 3. Screen shot of initial and final cell configurations for δ-Mo50-Ni.

Initial Configuration   Final Configuration

This and several other configurations were used to develop a simple free energy model of the Ni-Mo system by approximating the configuration entropy [54].

Lattice parameters: While current PPW codes can optimize supercell geometries by minimizing in the diagonal components of the stress tensor, it is still useful to know how to calculate the lattice parameters using equations of state. Perhaps the most cited equation of state used for this purpose was developed by F.D. Murnaghan in 1944 [55]. Assuming that the bulk modulus (K) is a linear function of the pressure:

Figure 4: Energy as a function of volume for fcc Ni calculated using VASP.
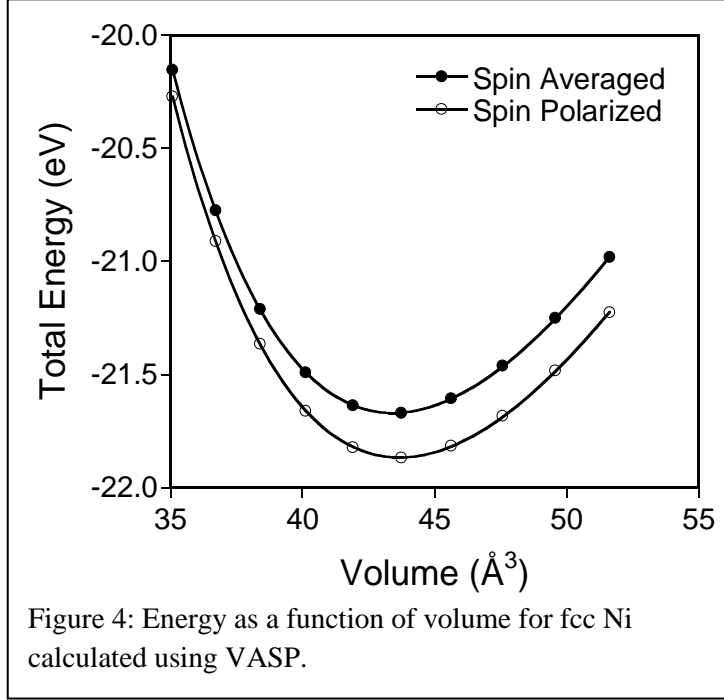
$$K = -V\frac{dP}{dV} = C(1 + kP)$$

(9)

Such that the bulk modulus (K) and its derivative at zero pressure respectively are identified as:

$$K(V_0) = -\left(V\frac{dP}{dV}\right)_{P=0} =$$
$$C \text{ and } \left(\frac{dK}{dV}\right)_{P=0} = -\frac{d}{dP}\left(V\frac{dP}{dV}\right)_{P=0} =$$
Ck respectively. Integrating equation (1) from zero pressure gives yields:
$P(V) = \frac{C}{Ck}\left(\left(\frac{V_0}{V}\right)^{Ck} - 1\right)$. Using
$P = -\frac{dE}{dV}$ we can identify $K = V\frac{d^2E}{dV^2}$
and finally:

$$V\frac{d^2E(V)}{dV^2} = C(1 + kP) = C\left(1 + k\frac{C}{Ck}\left(\left(\frac{V_0}{V}\right)^{Ck} - 1\right)\right) = C\left(\frac{V_0}{V}\right)^{Ck}$$

(10)

Integrating two times and identifying $C = K_0$ and $Ck = K_0'$ yields Murnaghan's equation of state (MES):

$$E(V) = E(V_0) + \frac{VK_0}{K_0'(K_0'-1)}\left[\left(\frac{V_0}{V}\right)^{K_0'} + K_0' - 1\right] - \frac{V_0K_0}{K_0'-1}$$

(11)

This somewhat complicated form can then be used to fit the energy as a function of volume calculated from electronic structure methods. For example Figure 4 shows the energy vs. volume for fcc Ni using PAW pseudopotentials and Table 6 gives the constants that produced the fitted curves.

In general DFT will predict low temperature lattice constants to within a percent. The LDA will typically underestimate lattice parameters, while the later improved gradient corrected approximations do not follow this trend[57]. MES also produces an estimate of the bulk modulus and its derivative with respect to volume. There are reasonable alternatives to MES such as the Birch form [58] that is favored in some applications [59].

Recent improvements to the gradient corrections that are designed to alleviate problems in low charge density regions (i.e. internal voids, surfaces and surfaces interactions) have produced mean errors in lattice parameters of approximately 0.1% over a wide range of materials [59].
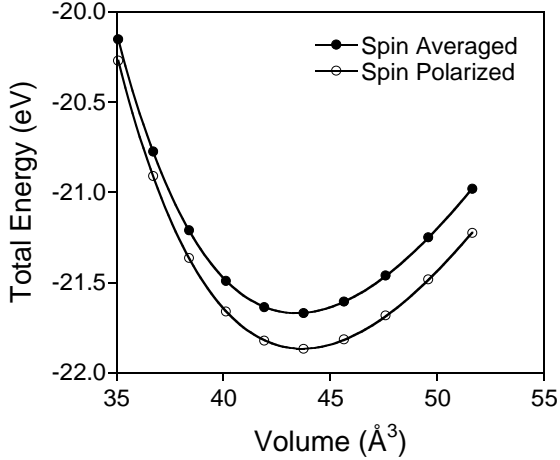
Figure 4: Variation in fcc-Ni cell energy as a function of volume calculated using VASP.

Table 6. Results of MES fit to VASP total energies for fcc-Ni.

	Ni -SA	Ni - SP	Exp.[56,51]
$E(V_0)$ (eV)	-21.67	-21.867	
K_0 (Mbar)	1.9681	1.9420	1.876
$K_0'\left(eV/\mathring{A}^6\right)$	4.7944	4.7628	
V_0 $(\mathring{A}^3)$	43.429	43.684	
a_0 (Å)	3.5150	3.5218	3.5238

Elastic Constants: One of the primary uses of DFT in crystalline metals has been to predict lattice parameters and elastic constants. Initially the calculations were used to assess the validity of the LDA and the computational methods. However, as the LDA became more established and the exchange-correlation functionals became more refined it became routine for groups to predict the Cij of simple metals. In the early 1990's DFT was used extensively to predict the elastic constants of a variety of high temperature intermetallics. Mehl and co-workers at the Naval Research Laboratory were one of the first groups to apply these methods and developed a robust strategy for assessing Cij for cubic and tetragonal crystal structures[60].

The general approach is to express the free energy of the system as a function of the strain tensor acting on a small simulation cell volume. We can start from: $dF = -SdT + PdV + dW$, where dW is the infinitesimal work done by elastically distorting the crystal. Specifically $dW = \sigma_{ij}d\epsilon_{ij} = C_{ijkl}\epsilon_{kl}d\varepsilon_{ij}$ where we have used the definition of the elastic constants relating the applied stress to the resulting strain: $\sigma_{ij} = C_{ijkl}\epsilon_{kl}$. Assuming reversible and isothermal loading at zero pressure: $dF = dW = C_{ijkl}\epsilon_{kl}d\epsilon_{ij}$ and we can write: $d^2F/d\epsilon_{ij}d\epsilon_{kl} = C_{ijkl}$. Changing notations from the fourth rank tensor to the reduced 2nd rank tensor [60] we express the energy of the system around equilibrium using a Taylor series expansion in the strain:

$$E(\epsilon) = E_0 - P(V_0)dV + \frac{V_0}{2}\sum_{i=1}^{6}\sum_{j=1}^{6}C_{ij}\epsilon_i\epsilon_j + \mathcal{O}(\epsilon^3) \qquad (12)$$

V and P(V) are the volume and pressure of the undistorted lattice, dV is the change in volume produced by the strain ϵ_i. It is natural to apply strains to the simulation cell by transforming the primitive lattice vectors of the cell using the strain tensor ε:

$$\begin{bmatrix} a_1' \\ a_2' \\ a_3' \end{bmatrix} = \begin{bmatrix} a_1 \\ a_2 \\ a_3 \end{bmatrix}(\mathbf{1} + \varepsilon) \; with \; \varepsilon = \begin{bmatrix} \epsilon_1 & \epsilon_6/2 & \epsilon_5/2 \\ \epsilon_6/2 & \epsilon_2 & \epsilon_4/2 \\ \epsilon_5/2 & \epsilon_4/2 & \epsilon_3 \end{bmatrix}$$

18

considering only non-rotating strains. Now for the specific case of cubic crystals where:

$$C_{ij} = \begin{bmatrix} C_{11} & C_{12} & C_{12} & 0 & 0 & 0 \\ C_{12} & C_{11} & C_{12} & 0 & 0 & 0 \\ C_{12} & C_{12} & C_{11} & 0 & 0 & 0 \\ 0 & 0 & 0 & C_{44} & 0 & 0 \\ 0 & 0 & 0 & 0 & C_{44} & 0 \\ 0 & 0 & 0 & 0 & 0 & C_{44} \end{bmatrix}$$ then the double summation in the equation for the energy as a

function of strain becomes:

$$\sum_{i=1}^{6} \sum_{j=1}^{6} C_{ij}\epsilon_i\epsilon_j = (\epsilon_1^2 + \epsilon_2^2 + \epsilon_3^2)C_{11} + 2(\epsilon_1\epsilon_2 + \epsilon_1\epsilon_3 + \epsilon_2\epsilon_3)C_{12} + (\epsilon_4^2 + \epsilon_5^2 + \epsilon_6^2)C_{44}$$

The effects of some applied strain are now explicitly coupled by elastic constants to changes in energy for a simulation cell with unit vectors $\boldsymbol{a}_i'$. For example, take the case of a hydrostatic stress of $\epsilon_1 = \epsilon_2 = \epsilon_3 = \delta$, this yields: $E(\epsilon) = E_0 + \frac{V_0}{2}\delta^2(3C_{11} + 6C_{12})$. Identifying the bulk modulus ($K = (C_{11} + 2C_{12})/3$) we find: $E(\epsilon) = E_0 + \frac{9}{2}V_0K\delta^2$. Applying this form to the data in Figure MES_PAW for the spin polarized case yields bulk modulus of 2.01 Mbar, in good agreement with MES.
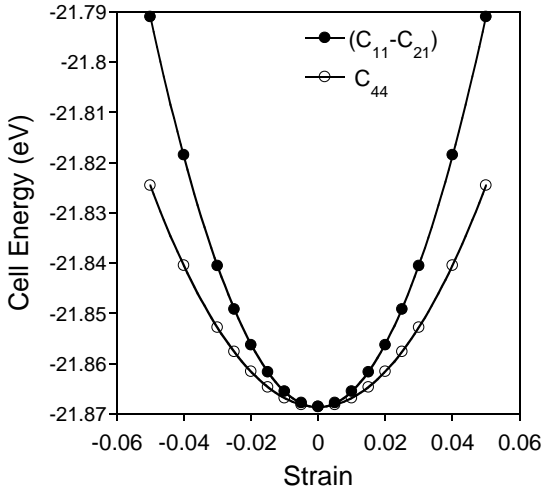
Figure 5: Calculation of Cij from volume conserving strains applied to fcc Ni calculated using VASP.

In order to find the three independent elastic constants two other equations are required, and the normal convention is to apply two other, volume conserving, strains. For cubic systems usually $C_{11} - C_{12}$ is found by applying $\epsilon_1 = -\epsilon_2 = \delta$, with ϵ_3 being set by the constant volume constraint for a cubic cell: $\epsilon_3 = \frac{\delta^2}{1-\delta^2}$. Similarly, C_{44} is found by setting $\epsilon_6 = \frac{\delta}{2}$ and $\epsilon_3 = \frac{\delta^2}{4-\delta^2}$. This yields two other equations for the energy as a function of strain:

$$E(\delta) = E_0 + V_0\delta^2(C_{11} - C_{12}) + \mathcal{O}(\delta^4)$$

$$E(\delta) = E_0 + \frac{V_0}{2}\delta^2 C_{44} + \mathcal{O}(\delta^4)$$

The response of a unit cubic cell of Ni to such strains is shown in Figure E_CIJ. When the fits to the two curves are combined with the MES results the elastic constants can be resolved as shown for fcc Ni and L1$_2$ Ni$_3$Al in Tables 2 and 3. The tabulated results are for spin averaged, spin polarized (ferro-magnetic), systems using LDA and GGA approximations. Tables 7 and 8 show the results from a PWPP calculation (VASP) using ultrasoft and projected augmented wave pseudopotentials respectively. Note that the LDA

and LSDA underestimate the lattice parameter and over estimate the elastic constants and the GGA results (PW91) show uniform improvement in lattice parameters and elastic constants. Finally, though PAW is assumed to be a better representation of the core states the USPP's produce a more accurate misfit parameter.

Table 7. Structural parameters for fcc Ni and $L1_2$ Ni_3Al calculated using ultrasoft pseudopotentials in a PWPP method (VASP). Spin averaged and spin polarized (ferromagnetic) calculations in the Local Density Approximation and a Generalized Gradient Approximation (PW91) are used to predict the lattice parameter (Angstrom), elastic constants (Mbar) and misfit parameter ($\delta = 2(a_{Ni_3Al} - a_{Ni})/(a_{Ni_3Al} + a_{Ni})$). As expected the LDA and LSDA underestimate the lattice parameters for Ni and Ni_3Al. GGA and SGGA produce significantly more precise lattice parameters and elastic constants, with the SGGA calculations giving the most accurate misfit parameter.

USPP		Spin Averaged				Spin Polarized				
Metal	Property	LDA	error	GGA	error	LSDA	error	SGGA	error	Exp[51,56]
Fcc	a_0 (Å)	3.4294	-2.7%	3.5258	0.1%	3.4221	-2.9%	3.5337	0.3%	3.5238
Ni	K	2.515	35%	1.985	6.8%	2.383	28%	1.962	5.5%	1.860
	C_{11}	3.154	27%	2.506	1.0%	3.034	22%	2.380	-4.1%	2.481
	C_{12}	2.195	42%	1.725	11%	2.057	33%	1.753	13%	1.549
	C_{44}	1.358	9%	1.057	-15%	1.363	10%	1.253	0.9%	1.242
	<err>		23%		6.8%		19%		4.8%	
$L1_2$	a_0 (Å)	3.4893	-2.2%	3.5769	0.3%	3.4928	-2.1%	3.5784	0.3%	3.5670
Ni_3Al	K	2.163	24%	1.777	2.1%	2.159	24%	1.787	2.7%	1.740
	C_{11}	2.749	21%	2.271	0.3%	2.778	23%	2.397	5.9%	2.264
	C_{12}	1.870	26%	1.529	3.3%	1.849	25%	1.481	0.1%	1.480
	C_{44}	1.431	11%	1.173	-8.7%	1.471	15%	1.240	-3.4%	1.284
	<err>		17%		2.9%		18%		2.5%	
	δ	0.0173	42%	0.0143	18%	0.0204	68%	0.0125	3%	0.0121

Table 8. Structural parameters for fcc Ni and $L1_2$ Ni_3Al calculated using Projected Augmented Wave pseudopotentials in a PWPP method (VASP). Spin averaged and spin polarized (ferromagnetic) calculations in the Local Density Approximation and a Generalized Gradient Approximation (PW91) are used to predict the lattice parameter (Angstrom), elastic constants (Mbar) and misfit parameter ($\delta = 2(a_{Ni_3Al} - a_{Ni})/(a_{Ni_3Al} + a_{Ni})$). As expected the LDA and LSDA underestimate the lattice parameters. For Ni and Ni_3Al, GGA and SGGA produce significantly more precise lattice parameters and elastic constants, with the SGGA calculations giving the most accurate misfit parameter.

PAW		Spin Averaged				Spin Polarized				
Metal	Property	LDA	error	GGA	error	LSDA	error	SGGA	error	Exp[51,56]

Fcc	a_0 (Å)	3.4197	-3.0%	3.5150	-0.2%	3.4258	-2.8%	3.5219	-0.1%	3.5238
Ni	K	1.144	-38%	1.968	5.8%	1.175	-37%	1.942	4.4%	1.860
	C_{11}	3.185	28%	2.480	0.0%	3.476	40%	2.704	9.0%	2.481
	C_{12}	2.227	44%	1.712	11%	2.019	30%	1.561	0.8%	1.549
	C_{44}	1.383	11%	1.121	-10%	1.618	30%	1.294	4.2%	1.242
	<err>		25%		5%		28%		4%	
L1$_2$	a_0 (Å)	3.4823	-2.4%	3.5685	0.04%	3.4927	-2.1%	3.5699	0.1%	3.5670
Ni3Al	K	2.183	25%	1.779	2.2%	2.171	25%	1.773	1.9%	1.740
	C_{11}	2.774	23%	2.264	0.0%	2.787	23%	2.343	3.5%	2.264
	C_{12}	1.888	28%	1.537	3.9%	1.863	26%	1.488	0.5%	1.480
	C_{44}	1.441	12%	1.189	-7.4%	1.488	16%	1.248	-2.8%	1.284
	<err>		18%		2.7%		18%		1.8%	
	δ	0.0181	49%	0.0151	24%	0.0193	59%	0.0135	11%	0.0121

Entropic contributions to the free energy: In the last 10 years significant progress has been made in calculating the entropic contributions to the free energy of bulk phases and defects. This includes configurational, vibrational and electronic entropic terms. Examples of applications, including references reviewing the techniques, are given here. Electronic entropy has been shown to be important in calculating defect energies, such as vacancies in body centered cubic metals[61]. Contribution of thermal vibrations to the free energy as a function of volume (harmonic and anharmonic terms) has been used to estimate the thermal expansion of a variety of metals[62,63]. Configurational entropy for dilute solute concentrations are treated using the Bragg Williams approximations in conjunction with either lattice gas models and the Low Temperature expansion[64,65]. For solid solutions at high concentrations cluster expansion methods[66,67] are used to approximate the free energy on an Ising model lattice. Recent progress in methods development has automated parts of the construction and use of these techniques[1,68]. Van de Walle and co-workers have also attempted to include all three entropic contributions in modeling phases stability and to inform CALculation of PHAse Diagram methods (CALPHAD)[69]. These developments have significantly improved the efficiency and accuracy of the Cluster Expansion approach, particularly in its application to phase diagrams.

References

[1] A. van de Walle and G. Ceder, The effect of Lattice Vibrations on Substitutional Alloy Thermodynamics, Rev. Mod. Phys., 74, 2002, p 11.
[2] A. Janotti, M. Krcmar, C.L. Fu and R.C. Reed, "Solute Diffusion in Metals: Larger Atoms Can Move Faster", Physical Review Letters, 92, 2004, p 085901.

[3] C. Woodward and S.I. Rao, "Flexible *Ab Initio* Boundary Conditions: Simulating Isolated Dislocations in bcc Mo and Ta"**,** Phys. Rev. Let., 88, 2001, p 216402.

[4] B. Grabowski, T. Hickel, J. Neugebauer, Phys. Rev. B 76, 2007, p 024309.

[5] D.J. Siegel, C. Wolverton, and V. Ozoliņš, Thermodynamic Guidelines for the Prediction of Hydrogen Storage Reactions and their Application to Destabilized Hydride Mixtures, Phys. Rev. B 76, 2007, p 134102.

[6] M. Ernzerhof and G.E. Scuseria, Assessment of the Perdew-Burke-Ernzerhof Exchange-Correlation Functional, J. Chem. Phys. 98, 199, p 5029-5036.

[7] P. Söderlind, L. Nordström, L. Tongming, and B. Johansson, "Relativistic Effects on the Thermal Expansion of the Actinide Elements", Phys. Rev. B 42, 1990, p 4544-4552.

[8] C. Woodward, D. R. Trinkle, L. G. Hector, Jr., and D. L. Olmsted, "Prediction of Dislocation Cores in Aluminum from Density Functional Theory", **100**, 2008, p 045507.

[9] W. M. C. Foulkes, L. Mitáš, R. J. Needs and G. Rajagopal. Quantum Monte Carlo Simulations of Solids, Rev. Mod. Phys. **73**, 2001, p 33–83.

[10] R. Martin, "Electronic Structure, Basic Theory and Practical Methods", Cambridge University Press**,** Cambridge, UK, 2004.

[11] M.C. Payne, M.P. Teter, D.C. Allen, T.A. Arias, and J.D. Joannopoulos, "Interative Minimization Techniques for Ab Initio Total Energy Calculations: Molecular Dynamics and Conjugate Gradients", Rev. Mod. Phys., **64**, 1992, p 1045-1097.

[12] D. Singh, "Planewaves, Pseudopotentials and the LAPW Method", Kluwer Academic Press, Norwell, Massachusetts, 1994.

[13] N.W. Ashcroft and N.D. Mermin, "Solid State Physics, Saunders College, Philadelphia, Pennsylvania, 1976.

[14] J. Hohenberg and L.J. Kohn, Phys. Rev., B136, 1962, p 864.

[15] W. Kohn and L.J. Sham, Self-Consistent Equations Including Exchange and Correlation Effects, Phys. Rev. 140, 1965, p 1133-1138.

[16] Pines, Elementary Excitations in Solids, Benjamin Inc. NY, 1963.

[17] Ceperly and Alder, Phys. Rev. Let. 45, 1980, p 566.

[18] Perdew and Zunger, Phys. Rev B23, 1981, p 5048.

[19] Moruzzi, J.F. Janak, and A.R. Williams, Calculated Electronic Properties of Metals, Pergamon, New York, 1978.

[20] J.C. Slater, Wavefunctions in a Periodic Potential, Phys. Rev. 51, 1937, p 846.

[21] J. M. Wills and B. R. Cooper, Phys. Rev. B **36**, 1987, p 3809; D. L. Price and D. R. Cooper, *ibid.* **39**, 989, p 4945.

[22] J. Korringa, Physica (Amsterdam), **13**, 1947, p 392; W. Kohn and N. Rostoker, Phys. Rev. **94**, 1954, p 1111; N. Papanikolaou, R. Zeller, P. H. Dederichs, and N. Stefanou, Comput. Mater. Sci. **8**, 19967, p 131.

[23] M Weinart, E. Wimmer, and A.J. Freeman, Total-energy All Electron Density Functional Method for Bulk Solids and Surfaces, Phys. Rev. B 26, 1982, p 4571-4578; H.J.F. Jansen and A.J. Freeman, Total Energy Full Potential Linearized Augmented-Planewave Method for Bulk Solids, Phys. Rev. B 30, 1984, p 561-569.

[24] J.M. Wills and B.R. Cooper, Phys. Rev. B 36, 1987, p 3809; K.H. Weyrich, Full Potential Linear Muffin-tin Orbital Method, Phys. Rev. ,B 37, 1988, p 10269-10282.

[25] F. Herman, Theoretical Investigation of the electronic energy band structure of solids, Rev. Mod. Phys., 30, 1958, p 102.

[26] N. Troullier and Jose Luis Martins, Phys. Rev. B43, 1991, p 1993.

[27] D. Vanderbilt, Phys. Rev., B41, 1990, p 7892.

[28] P.E. Blochl, Phys. Rev. B 50, 1994, p 17953.

[28b] M. Marsman and G. Kresse, J. Chem. Phys., 125, 2006, p 104101.

[29] R. Feynman, Phys. Rev., 56, 1939, p 340.

[30] O.H. Nielsen and R.M. Martin, Phys. Rev., B32, 1985, p 3780.

[31] S. Y. Savrasov, D.Y. Savrasov, and O.K. Anderson, Linear Response Calculations of Electron-Phonon Interactions, Phys. Rev. Lett., 72, 1994, p 372-375.

[32] Carr and Parrinello, Phys. Rev. Lett., 55, 1985, p 2471-75.

[33] M.P. Teter, M.C. Payne and D.C. Allan, Phys. Rev., B40, 1989, p 12255.

[34] International Tables for Crystallography. Volume A, Space-group Symmetry (5th edition, ed. Theo Hahn ed.). Dordrecht: Kluwer Academic Publishers , 2002.

[35] D.J. Chadi and M.L. Cohen, Phys. Rev. B **8**, 1973, p 5747.

[36] H.J. Monkhorst and J.D. Pack, Phys. Rev. B **13**, 9765, p 188.

[37] M. Weinert and J. W. Davenport, Phys. Rev. B 45, 1992, p 13709.

[38] C.-L. Fu and K.-M. Ho, First Principles Calculations of the Equilibrium Ground State Properties of Transition Metals: Application to Nb and Mo, Phys. Rev. B28, 5480-.5486 (1983); C. Elsasser, M. Fahnle, C.T. Chan, and K.M. Ho, Density-Functional Energies and Forces with Gaussian-broadened Fractional Occupancies, Phys. Rev. B 49, 1994, p 13975.

[39] See for example, D. J. Singh, *Planewaves, Pseudopotentials and the LAPW Method*, (Kluwer Academic Press, 1994), p 66.

[40] F. Nogueiray, C.Fiolhaisy, J. Hez, J. P Perdew and A. Rubio, Transferability of a Local Pseudopotential based on Solid State Electron Density, J. Phys.: Condens. Matter, 8, 1996, p 287-302.

[41] Y. A. Wang and E. A. Carter, in *Theoretical Methods in Condensed Phase Chemistry*, ed. S. D. Schwartz, within the series "Progress in Theoretical Chemistry and Physics," Kluwer, Dordrecht, 2000, pp. 117–184.

[42] W. Kohn, Rev. of Mod. Phys., 71, 1999, p 1253.

[43] J.P. Perdew, in Electronic Structure of Solids'91, ed. P. Ziesche and H. Eschrig Akademie-Verlag, Berlin, 1991; J.P. Perdew, J.A. Chevary, S.H. Vosko, K.A. Jackson, M.R. Pederson, D.J. Singh, and C. Fiolhais, Phys. Rev. B 46, 1992, p 6671.

[44] V. Ozoliņš and M. Körling, Full Potential Calculations Using the Generalized Gradient Aproximation: Structural Properties of Transition Metals, Phys. Rev. B 48, 1993, p 18304-18307.

[45] T.C. Leung, C.T. Chan and B.N. Harmon, Phys. Rev. B44, 1991, p 2923.

[46] J-H. Cho and M. Scheffler, Phys,. Rev. B53, 1996, p 10685.

[47] J.P Stevens, F.J. Devlin, C.F. Chablowski, M.J. Frisch, J. Phys. Chem, 80, 1994, p 11623; A.D. Becke, J. Chem. Phys., 98, 1993, p 5648.

[48] A.E. Mattsson, R. Armiento, J. Paier, G. Kresse, J.M. Wills and T.R. Mattsson, Journ. Chem. Phys. 128, 2008, p 084714.

[49] G. Kresse and J. Furthmüller, Efficiency of *ab-initio* total energy calculations for metals and semiconductors using a plane-wave basis set, Comput. Mat. Sci. 6, 1996, p 15-50.

[50] G. Kresse and J. Furthmüller, Efficient iterative schemes for *ab initio* total-energy calculations using a plane-wave basis set, Phys. Rev. B **54**, 1996, p 11169.

[51] W. B. Pearson, A Handbook of Lattice Spacings and Structures of Metals and Alloys, N.Y.: Pergamon Press, 1967; also see http://cst-www.nrl.navy.mil/lattice/index.html

[52] Online Bilbao crystallographic server: http://www.cryst.ehu.es/

[53] C.B. Shoemaker and D. P. Shoemaker, "Crystal Structure of the d Phase, Mo-Ni", Acta Crys., 16, 1963, p 997.

[54] Y. Wang, C. Woodward, S.H. Zhou, Z.-K. Liu, L.-Q. Chen, Structural Stability of Ni–Mo Compounds From First-Principles Calculations, Scripta Met., 52, 2005, p 17-20.

[55] F.D. Murnaghan, Proc. Nat. Acad. Sci., USA, 30, 1944, p 244.

[56] G. Simmons and H. Wang, Single Crystal Elastic Constants, Cambridge MA: MIT Press, 1971.

[57] P. Söderlind, O. Eriksson, J.M. Wills, and A.M. Boring, Theory of Elastic Constants of Cubic Transition Metals and Alloys, Phys. Rev. B 48, 1993, p 5844-5851

[58] F. Birch, J. Geophys. Res. 83, 1978, p 1257.

[59] M.J. Mehl, J.E. Osborn, D.A. Papaconstantopoulos, and B. M. Klein, Phys. Rev. B41, 1990, p 10311-10323.

[59] A.E. Mattsson, R. Armiento, J. Paier, G. Kresse, J.W. Wills, and T.R. Mattsson, Journ. Chem. Phys., 128, 2008, p 084714.

[60] J.F. Nye, Physical Properties of Crystals, Clarendon Press, Oxford 1987.

[61] A. Satta, F. Willaime, S. de Gironcoli, First Principles Study of Vacancy FOramtion anfd Migration Energies in Tantalum, Phys. Rev. B, 60, 1999, p 7001-5; A. Satta, F. Willaime, S. de Gironcoli, Vacncy Self-Diffusion in Tungston: Finite Electron-Temperature LDA Calcaultions, Phys. Rev., B 57, 1998, p 11184-92

[62] V.L. Moruzzi, J.F. Janak, and K. Schwarz, Phys. Rev. BG 37, 1988, p 790.

[63] P. Söderlind, L. Nordström, L. Yongming, and B. Johansson, Phys. Rev., B 42, 1990, p 4544.

[64] J. Mayer, C. Elsasser, and M. Fahnle, Phys. Stat. Solidi, B 191, 1995, p 283.

[65] C. Woodward, M. Asta, G. Kresse, and J. Hafner, Density of Constitutional and Thermal Point Defects in $L1_2$ Al_3Sc, Phys. Rev., B 63, 2001, p 094103.

[66] J.M. Sanchez, F. Ducastelle, D. Gratis, Physica A, 128, 1984, p 334.

[67] D. de Fontaine, Configurational Thermodynamics of Solid Solutions, in *Solid State Physics* Academic Press, New York, 1979, Vol. 34, p 73.

[68] A. van de Walle, M. Asta, G. Ceder, The Alloy Theoretic Automated Toolkit: A User Guide, Calphad, **26**, 2002, p 539-553.

[69] van de Walle A, Ghosh G, Asta M. Ab initio Modeling of Alloy Phase Stability, in Applied Computational Materials Modeling: Theory, Simulation and Experiment, Ed. by G. Bozzolo, R.D. Noebe, and P. Abel, New York: Springer; 2007, p 1–34.

Selected References

R. Martin, "Electronic Structure, Basic Theory and Practical Methods", Cambridge University Press, Cambridge, UK, 2004.

M.C. Payne, M.P. Teter, D.C. Allen, T.A. Arias, and J.D. Joannopoulos, "Interative Minimization Techniques for Ab Initio Total Energy Calculations: Molecular Dynamics and Conjugate Gradients", Rev. Mod. Phys., **64**, 1992, p 1045-1097.

D. Singh, "Planewaves, Pseudopotentials and the LAPW Method", Kluwer Academic Press, Norwell, Massachusetts, 1994.

J.C. Slater, Quantum Theory of Matter, McGraw Hill, New York, NY, 1968.

J.C. Slater, Quantum Theory of Molecules and Solids, Vol. 1-2, McGraw Hill, New York, NY, 1974.